geoconvention
Calgary • Canada • May 12-14 2025

Geochemical Modelling of Carbon Sequestration

Maurice T. Shevalier
Montrose Environmental

Introduction

Carbon Capture and Storage is fast becoming a new industry in western Canada, especially in Alberta. Carbon storage, i.e. the geological sequestration of CO_2 in saline aquifers, has been shown to be a safe and permanent method for large scale CO_2 mitigation. The Western Canada Sedimentary Basin (WCSB) has been shown to have the right geological condition for long term sequestration of CO_2 (Bachu et al., 1994; Gunter et al., 1993, 1996, 1997). The Alberta Basin capacity for CO_2 storage was estimated to be approximately 8.3Gt (White et al., 2003) Under the recently released Directive 65 (Alberta, 2024) to understand and predict the fate and potential impacts of CO_2 injection into saline aquifers, flow modelling, geomechanical modelling, and geochemical modelling need to be conducted. All these models play an important role in understanding and predicting the fate and potential impacts of injected CO_2 on the saline aquifer.

Geochemical modelling of injected CO_2 into a saline aquifer is important in determining the geochemical reactions that can occur in the reservoir. Changes in mineral compositions from reactions between injected CO_2 and reservoir minerals can result in changes to porosity and permeability of the reservoir. Further reactions between the caprock and injected CO_2 may result in changes to the structure of the caprock.

. A common program used in this type of geochemical modelling is TOUGHREACT, a program designed at the Lawrence Berkley National Laboratory. It is a multiphase reactive-transport code based on TOUGH2 and can be used to simulate a number of problems in porous and/or fractured media, including geological storage of CO_2 in deep formations. An example of potential geological storage of CO_2 in a saline reservoir, and CO_2 storage in the Devonian Nisku formation in central Alberta, is presented and shows the changes in reservoir porosity, permeability and mineralogy within the storage reservoir.

Geochemical Storage and Geochemical Reactions

CO_2 is retained in geological formations in four possible ways (Hitchon, 1996). The first method is that CO_2 can be trapped as a supercritical fluid under a low permeability caprock. This process is commonly known as “hydrodynamic trapping” and will be the most important method of retention. A second method involves trapping of supercritical CO_2 in small pore regions makes it essentially immobile and is known as “residual trapping”. The third method is where CO_2 can dissolve in the water and this process is known as “solubility trapping”. This method increases the acidity of the water and increases the solubilities of many minerals composing the host rock matrix. The fourth method is where CO_2 directly or indirectly reacts with minerals in the storage formation leading to the precipitation of secondary minerals. This is known as “mineral trapping” (Bachu et al., 1994) and is attractive for long term storage of CO_2. The dissolution of alkaline aluminosilicate minerals by CO_2 would increase the concentration of soluble carbonates and bicarbonates in solution thereby enhancing “solubility trapping”.

After injection, some supercritical CO_2 will initially remain in free phase and will be subject to hydrodynamic or residual trapping in the reservoir. However, supercritical CO_2 will undergo a number of chemical processes, such as CO_2 dissolution in the brine. During dissolution of CO_2 in the brine, the supercritical CO_2 phase and the aqueous phase are assumed to be in equilibrium:

$$CO_{2(sc)} \leftrightarrow CO_{2(aq)} \quad \text{Reaction (1)}$$

Where "sc" and "aq" subscripts denote supercritical and aqueous CO_2, respectively. This process results in solubility trapping of injected CO_2. The aqueous CO_2 phase, $CO_{2(aq)}$, reacts with water forming carbonic acid (H_2CO_3) and this acid dissociates into a proton (H^+) and bicarbonate ion (HCO_3^-) resulting in the decrease in pH and acidification of the brine.

$$CO_{2(aq)} + H_2O \leftrightarrow H_2CO_3 \quad \text{Reaction (2)}$$

$$H_2CO_3 \leftrightarrow H^+ + HCO_3^- \quad \text{Reaction (3)}$$

Furthermore, carbonic acid may react with any mineral present in the formation such as calcite and albite releasing cations (e.g. Ca^{2+} and Na^+).

$$H_2CO_3 + CaCO_3 \leftrightarrow Ca^{2+} + 2HCO_3^- \quad \text{Reaction (4)}$$

$$NaAlSi_3O_8 + 4H^+ + 4H_2O \leftrightarrow Na^+ + Al^{3+} + 3H_4SiO_4 \quad \text{Reaction (5)}$$

Dissolution of primary minerals may increase the aqueous concentrations of cations such as Ca^{2+}, Mg^{2+} and Fe^{2+}, which can lead to precipitation of secondary carbonate minerals such as dawsonite, siderite and ankerite. This process results in CO_2 mineral trapping, the most stable long-term form of geological carbon sequestration.

$$Na^+ + Al^{3+} + HCO_3^- + 2H_2O \leftrightarrow NaAl(CO_3)(OH)_2 + 3H^+ \quad \text{Reaction (6)}$$

Numerical modelling is an important tool that can give insights into the likelihood of the occurrence of these geochemical reactions induced by CO_2 injection into complex geological environments during CO_2 storage projects and beyond.

Numerical Modelling Approach

The simulations were carried out using the non-isothermal reactive geochemical transport code TOUGHREACT (Xu and Pruess, 1998, 2001). The code was developed by introducing reactive chemistry into the framework of the existing multi-phase fluid and heat flow code TOUGH2 (Pruess, 1991). The flow and transport in geological systems are based on space discretization via integral finite differences (Narasimhan and Witherspoon, 1976). For the individual components of the model consisting of flow, transport and geochemical reactions an implicit time-weighted scheme is used. A sequential iteration approach where transport and reaction equations are solved separately is used in TOUGHREACT.

Local equilibrium is assumed to govern the aqueous chemical species distribution. Given that homogeneous reactions in an aqueous phase can be almost instantaneous, they can be considered to be at equilibrium.

Mineral dissolution/precipitation is subject to either local equilibrium or kinetic conditions. The general rate equation used in TOUGHREACT is taken from Lasaga et al. (1994):

$$r_n = \pm k_n A_n \left|1 - \left(\frac{Q_n}{K_n}\right)^{\theta}\right|^{\eta}$$ Equation (1)

Where n is the kineric mineral index, positive values of r_n indicate dissolution and negative values indicate precipitation, k_n is the rate constant (moles per unit mineral surface area and unit time) which is temperature dependent, A_n is the specific reactive surface area per kilogram of water,, K_n is the equilibrium constant for the mineral-water reaction for one mole of mineral n, and Q_n is the reaction quotient. Parameters θ and η are experimental derived and can be taken to be equal to one.

For many minerals the kinetic rate constant k can be the sum of three mechanisms, neutral (nu), acid (H), and base mechanisms (OH) (Palandri and Kharaka, 2004):

$$k = k_{25}^{nu} exp\left[\frac{-E_a^{nu}}{R}\left(\frac{1}{T} - \frac{1}{298.15}\right)\right] + k_{25}^{H} exp\left[\frac{-E_a^{H}}{R}\left(\frac{1}{T} - \frac{1}{298.15}\right)\right] a_H^{n_H} + k_{25}^{OH} exp\left[\frac{-E_a^{OH}}{R}\left(\frac{1}{T} - \frac{1}{298.15}\right)\right] a_{OH}^{n_{OH}}$$

Equation (2)

where E_a is the activation energy, k_{25} is the rate constant at 25 °C, R is the universal gas constant, T is the absolute temperature, a is the activity of the species and n is an exponent (constant).

CO_2 solubility is defined in a fluid property module, ECO2N, which comprehensively describes the thermodynamic and thermophysical properties of H_2O-NaCl-CO_2 mixtures. The module reproduces the fluid properties, within experimental error, for the temp, pressure and salinity conditions of interest, i.e., 10 °C ≤ T ≤ 110 °C; P ≤ 600 bar; salinity up to full halite saturation. It can model flow processes isothermally or non-isothermally and phase conditions that are represented can include a single (aqueous or CO_2-rich) phase as well as two phase mixtures. It can also model super- as well as sub-critical conditions. However, it does not make a distinction between liquid and gaseous CO_2 and thus is not applicable for processes that involve two CO_2-rich phases.

Model Setup

A 2-D radially symmetric model was developed to simulate CO_2 injection into the Nisku aquifer in which the effects of gravity were taken into account. The 2-D model contains the Nisku aquifer with its caprock, Calmar Formation and the bottom rock, Ireton Formation. The vertical extent of the model is 90 m composed of 36 layers of 2.5 m thickness. The lowermost 10 m of the model represent the Ireton Formation, followed by 70 m of Nisku aquifer capped by 10 m of the Calmar caprock (Figure 1). The radial distance of the 2-D model was 20,000 m divided into 100 cells with non-uniform spacing increasing gradually from the injection well. The first cell has a radius of 10 m. The outermost cells were set numerically very large so that the model can act infinite. The 2-D model is composed of 3600 cells (36 cells in vertical and 100 cells in radial directions). The CO_2 was injected into the bottom 10 m of the Nisku Formation.

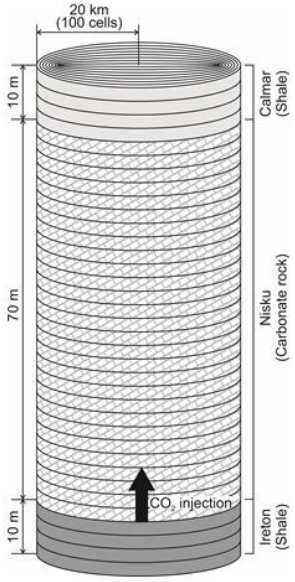

Figure 1. 2-D Model representation of the Nisku aquifer with Calmar caprock and Ireton bottom rock.

The overlying Calmar caprock of the Nisku Formation has a very low permeability of 2.9 x 10^{-6} mD. The porosity of the Calmar caprock is around 4% (Bennion and Bachu, 2007). The Nisku aquifer is a homogeneous formation with an average porosity and permeability of circa 20% and 91 mD. The underlying Ireton Formation has an average porosity of 5% and an average permeability of 0.1 mD and is hence more permeable than the Calmar shale. Each formation defined in the 2D model was assumed to be isotropic and homogeneous in terms of porosity and permeability.

The initial mineral compositions of representative samples from the Calmar, Nisku and Ireton Formations used in the modeling are from Nightingale et al. (2009). Quantitative mineralogy was determined using linear programming normative analysis (LPNORM). LPNORM incorporates mineralogical information from several sources such as thin section, XRD and electron microprobe with whole-rock analysis such as XRF (De Caritat et al., 1994). The Calmar Formation is composed of mainly quartz (48.2%), illite (29.3%), K-feldspar (17.3%) and minor amounts of low-albite, pyrite and calcite. The Nisku is a carbonate formation, consisting of mostly dolomite (81.2%), calcite (15.5%) and small amounts of illite, K-feldspar and low-albite. The Ireton Formation is composed of illite (40%), calcite (27.4%), quartz (9.8%), K-feldspar (8.4%) and minor amounts of dolomite, chlorite, low-albite and pyrite.

The measured brine composition was taken from a sample obtained from a water-producing well located in the Nisku Formation and is shown in Table 1 (Shevalier and Mayer, 2009). The total dissolved solids (TDS) were measured to be approximately 195,000 mg/L for formation water from this well. TDS values in the Nisku Formation vary from less than 125,000 and more than 200,000 mg/L, increasing in the southwestern part of the formation (Lavoie and Keith, 2010).

Table 1: Water analysis of produced water.

Analyte	Concentration (mg/L)	Analyte	Concentration (mg/L)
pH	6.4	Sr^{2+}	884
Ca^{2+}	0.41	HCO_3^-	577
Mg^{2+}	2129	SO_4^{2-}	470
Na^+	55,150	Cl^-	117,743
K^+	3720	SiO2	25.68

Before commencement of reactive transport modeling using the code TOUGHREACT, batch modeling without CO_2 injection was performed for a time period of 50 years to equilibrate the formation water (Table 1) with the primary minerals present in each formation. This resulted in the initial formation water chemistries for the Calmar, Nisku and Ireton Formations prior to CO_2 injection that are summarized in Table 2.

Table 2: Initial water chemistry used in the TOUGHREACT simulations

Analyte	Concentration (mol/kg)		
	Calmar	Nisku	Ireton
AlO_2^-	1.21E-8	5.7e-11	9.8e-9
Ca^{2+}	0.372	0.0162	0.0154
Cl^-	1.99	1.99	1.99
Fe^{2+}	1.41e-13	6.73e-7	9.14e-15
HCO_3^-	1.16E-5	0.0144	1.13e-4
K^+	0.0114	0.0947	0.0082
Mg^{2+}	0.0838	0.4590	0.4370
Na^+	1.22	1.10	1.23
O_2(aq)	-0.0019	2.24e-21	-0.0098
SiO_2(aq)	0.0019	0.0036	0.0021
SO_4^{2-}	0.0061	0.0050	0.0106
Sr^{2+}	0.0102	0.0102	0.0102
pH	8.5	6.4	8.5

The initial reservoir temperature and pressure was 70°C and 17.5 MPa. Thus, the injected CO2 was in a supercritical state and injected into the bottom 10 m of the Nisku Formation at a rate of 1 Mton/year (31.69 kg/s) for 50 years. The simulations were performed using TOUGHREACT v. 1.2 (Xu and Pruess, 2001) and isothermal condition was assumed.

Results

2D radial modeling of CO_2 injection into the Nisku aquifer was performed for an injection period of 50-years with a post-injection period of 1000 years. The simulation results are presented in 2-D plots as a function of depth and radial distance at discrete time intervals of 1, 25 and 50 years of CO_2 injection and 100, 500 and 1000 years of post-injection. The discrete time intervals were chosen to represent the beginning, mid and final periods of CO_2 injection and storage phases.

CO_2 injection

The initial reservoir pressure in the Nisku aquifer before CO_2 injection was 17.5 MPa. Once CO_2 injection began the pressure of the Nisku Formation started to increase with the maximum

pressure around the injection region of ~20 MPa at the end of the 50 years of injection. Thus, CO_2 injection at a high rate of 1 Mt annually (31.69 kg/s) did not induce a formation pressure that exceeds the fracture pressure of the Nisku Formation that has been reported to be higher than 30 MPa (Lavoie and Keith, 2010). While fracturing the Nisku storage reservoir may increase the injectivity and CO_2 storage capacity, it may also impact the caprock, although the Calmar has a higher fracturing strength than the Nisku Formation (Lavoie and Keith, 2010).

The calculated brine density of the Nisku was ~1150 kg/m^3 with the density of the supercritical CO_2 calculated at ~600 kg/m^3 (Clifford, 2007) at the Nisku temperature and pressure. Thus, the supercritical CO_2 was significantly less dense than the brine. Therefore, the injected CO_2 not only spread radially around the injector but also tended to migrate upwards due to buoyancy-driven force until reaching the Calmar caprock. CO_2 migrated towards the Calmar caprock and started forming a CO_2 plume beneath this caprock after 1 year of injection (Figure 2a). The top of the CO_2 plume reached a radial extent of 0.5, 2.5 and 3.5 km, respectively at after 1, 25 and 50 years of injection (Figures 2a–c). The bottom of the CO_2 plume extended 0.25, 0.4 and 0.5 km from the injection well, respectively, after 1, 25 and 50 years of injection. During the first 25 years of injection, no injected CO_2 was observed to intrude into the Calmar shale. After 50 years, however, a minor amount of injected CO_2 diffused into the two bottommost layers of the Calmar caprock reaching average CO_2 saturations of ~0.28. The injected supercritical CO_2 started also migrating down around the injection well to the underlying Ireton shale after 1 year of CO_2 injection as the Ireton Formation is more porous and permeable than the Calmar caprock. After 25 and 50 years, the supercritical CO_2 saturation in the Ireton Formation reached an average value of 0.5 (Figures 2b and c).

As supercritical CO_2 is injected into the reservoir it displaces formation brine that initially occupies the pores. This caused a dehydrated region indicated by supercritical CO_2 saturation values approaching 1.0 around the injection well. After 1 year of injection, this dehydration region was 10 m thick extended radially up to 100 m around the injection well (Figure 2a). Its thickness increased up to 60 m after 25 years and 70 m after 50 years of injection, covering the entire thickness of the Nisku Formation (Figure 3a and b). The lateral extent of this region remained constant with up to 80 m after 25 and 50 years of injection.

Figures 3a–c shows the spatial and temporal distribution of mass fraction of dissolved CO_2, $XCO_2(aq)$ (mass of CO_2 dissolved by mass of aqueous phase), concentration of HCO_3^-, and the pH value after 1, 25 and 50 years of injection. After 50 years of injection, the dissolution of supercritical CO_2 in the brine produced a maximum dissolved CO_2 mass fraction of ~0.04. The dissolved CO_2 mass fraction in the Nisku aquifer before injection was negligible with $<1.0 \times 10^{-5}$. According to reactions (1–3), the dissolution of injected supercritical CO_2 into the Nisku brine caused an increase in the concentration of HCO_3^- to around 1.3 mol/kg from its initial value of 0.014 mol/kg during the injection (Figure 3b). Increases in the spatial extents of $XCO_2(aq)$ and HCO_3 concentrations in the brine were observed due to mixing and convection of CO_2-saturated and CO_2-unsaturated brines over the simulation period. The brine pH decreased to values as low as 5.0 from its initial value of 6.4 in the Nisku aquifer (Figure 3c).

As supercritical CO_2 entered into the Ireton Formation (Figure 2), some CO_2 dissolution occurred in the Ireton brine. The maximum dissolved CO_2 mass fraction was ~0.04 in the Ireton brine after 50 years (Figure 4a). The HCO_3^- concentration in the Ireton brine also increased to 1.2 mol/kg

from its initial value of 0.0001 mol/kg (Figure 3b). Due to dissolution of the supercritical CO_2, the pH decreased from its initial value of 8.5 to ~5.1, 5.0 and 5.0 in the fluids in the affected part of the Ireton Formation after 1, 25 and 50 years of injection.

In the Calmar caprock, no major change in the $XCO_2(aq)$ and HCO_3^- concentration were observed during CO_2 injection. In the small areas affected by minor CO2 diffusion into the bottom of the caprock, the pH decreased to ~6.0 from its initial value of 8.5.

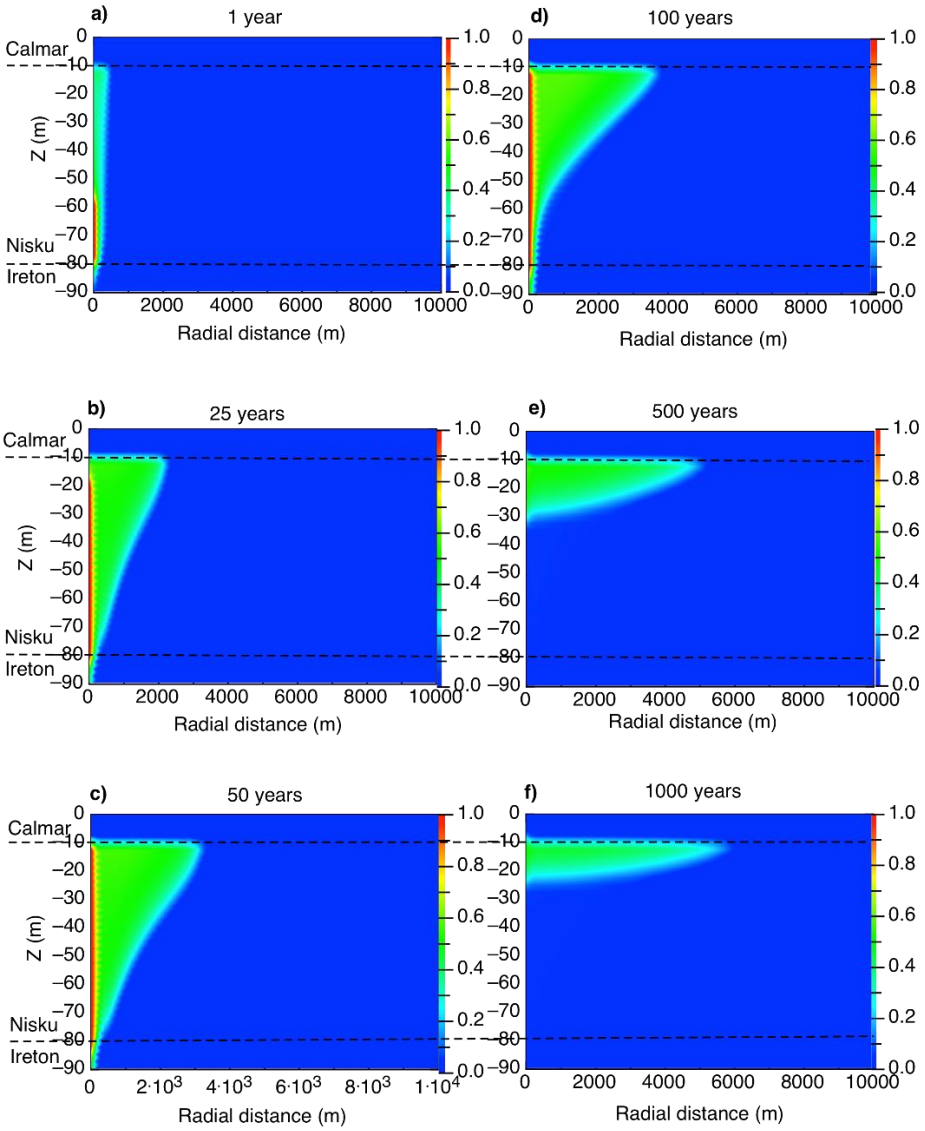

Figure 2: Spatial Distribution of supercritical CO_2 saturation during **(a-c)**1-, 25- and 50-years of injection **(d-f)** 100-, 500- and 1000-years post-injection.

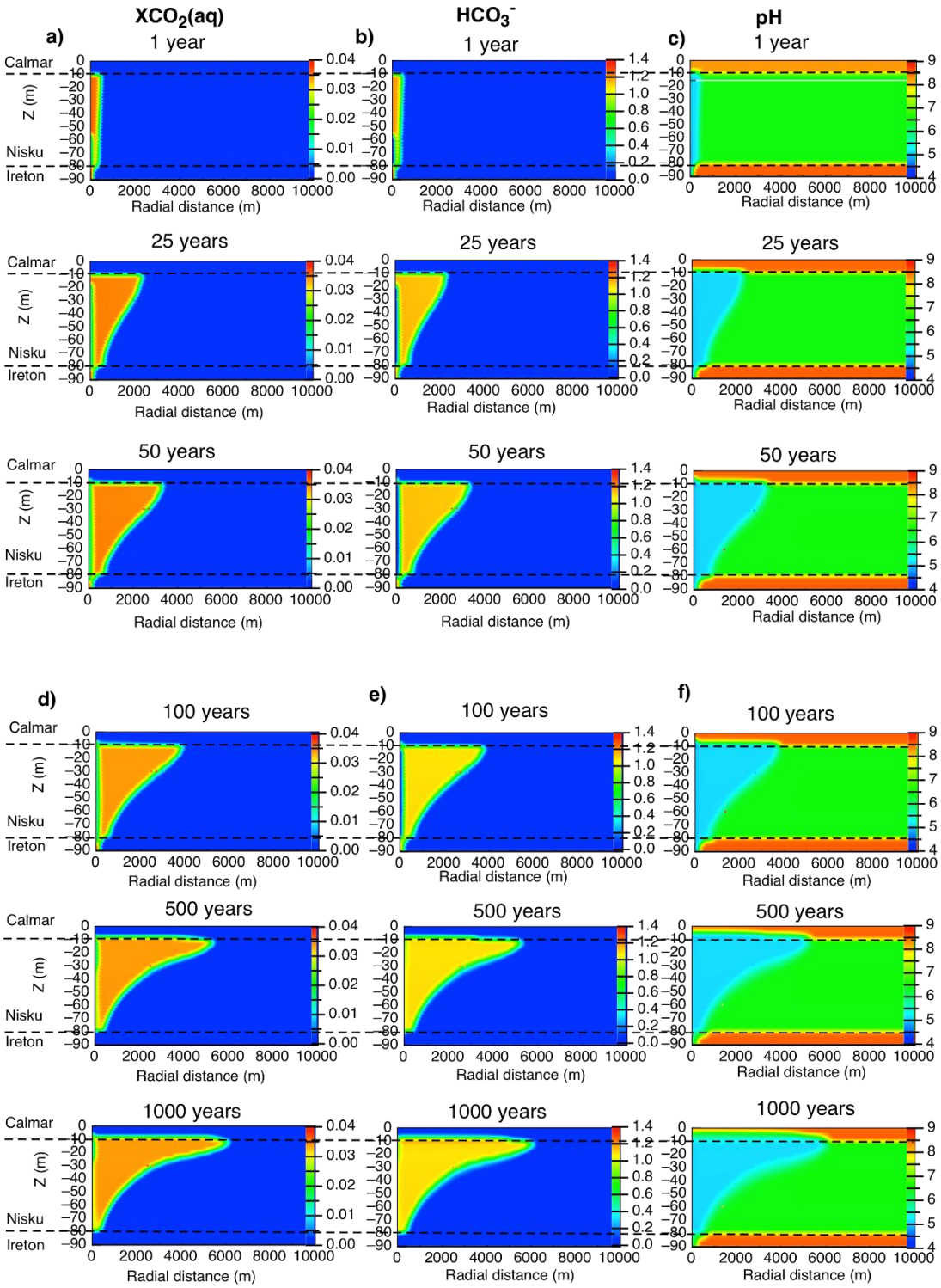

Figure 3: Spatial distribution of **(a–c)** dissolved CO_2 mass fraction, $XCO_2(aq)$, concentration HCO_3 (mol/kg) and pH during injection and **(d–f)** $CO_2(aq)$, HCO_3 and pH during post injection.

Post-Injection

It has been reported that injected CO_2 in free phase in the reservoir can take several thousand years before it completely dissolves in brine (Lindeberg and Bergmo, 2002). Therefore, an evaluation was done to determine how long CO_2 remains as a free-phase in the reservoir and how much of the injected CO_2 dissolved. This determines the timescale over which a free-phase CO_2 can potentially leak from the storage reservoir. As illustrated in Figures 2d–f, the supercritical CO_2 saturation was ~0.5 at the end of 1000 years of post-injection, and the plume had accumulated mainly in the upper 20 m and 15 m of the Nisku aquifer under the Calmar caprock after 500 and 1000 years respectively driven by buoyancy force. The CO_2 plume that had extended radially to 3.5 km after 50 years of injection, reached ~6.0 km in the Nisku storage aquifer after 1000 years of post-injection (Figure 2f). Due to buoyancy, the injected supercritical CO_2 migrated up into the bottom two layers (=5 m) of the Calmar shale. The maximum CO_2 saturation in these two layers was around 0.5 after 1000 years. It was also observed that CO_2 had migrated down into the Ireton shale during the 50-year injection period, but after 500 years of post-injection no supercritical CO_2 remained in the Ireton Formation suggesting complete CO_2 dissolution in the brine (Figures 2e and f).

Figures 3d–f shows the spatial and temporal distributions of mass fraction of dissolved CO_2, $XCO_2(aq)$, concentration of HCO_3 and the pH value in brines after 100-, 500- and 1000-years post-injection. A small, dehydrated region had formed in the vicinity of the injection well during the injection phase because of the high rate of injection (31.69 kg/s) (Figures 2a–c). Although injection ceased after 50 years, this dehydrated region remained after 100 years (Figure 2d) but disappeared after 500 years (Figure 2f) since the brine, which had been previously displaced during injection, returned due to capillary effects when the supercritical CO_2 migrated up due to buoyancy.

Solubility trapping of CO_2 continued to increase as the spatial extent of the mass fraction of dissolved CO_2, $XCO_2(aq)$, increased with time due to convective mixing of brine. The mass fraction of dissolved CO_2 was ~0.04 during the 1000-year post-injection period (Figure 3d). The concentration of HCO_3 remained ~1.3 mol/kg during the 1000-year post-injection period (Figure 3e). The pH value remained at ~5.0 due to dissolution of the supercritical CO_2 in the region of the Nisku aquifer affected by the CO_2 injection although dolomite dissolution was also buffering the pH.

Figure 4 shows the spatial distribution of the CO_2 sequestered via mineral trapping. Negative values indicate mineral dissolution, and positive values suggest CO_2 storage via mineral precipitation. Extensive dissolution of dolomite was observed in the Nisku aquifer. Secondary calcite precipitation was observed coupled with dolomite dissolution. However, since dolomite dissolution was dominant over calcite precipitation, no net-storage of injected CO_2 occurred through mineral trapping in the Nisku saline aquifer. This indicates that the Nisku aquifer has negligible mineral trapping capacity for CO_2. This suggests that the dominant CO_2 trapping mechanisms in the Nisku Formation are solubility and hydrodynamic trapping. The capacity to sequester injected CO_2 in mineral form was highest in the Ireton Formation, with mineral trapping of 2, 8 and 14 kg of the injected CO_2 per m3 of rock after 100, 500 and 1000 years respectively, indicating that the Ireton Formation has a large CO_2 mineral trapping capacity (Figure 4). The Ireton Formation contains aluminosilicate minerals, resulting in injected CO_2 sequestered as

ankerite and dolomite, the reaction products of rock–water–CO_2 reactions. The total amount of CO_2 sequestered in form of these carbonates was negligible in the Ireton Formation. No CO_2 was observed being sequestered by mineral trapping (as carbonates) in the Calmar caprock.

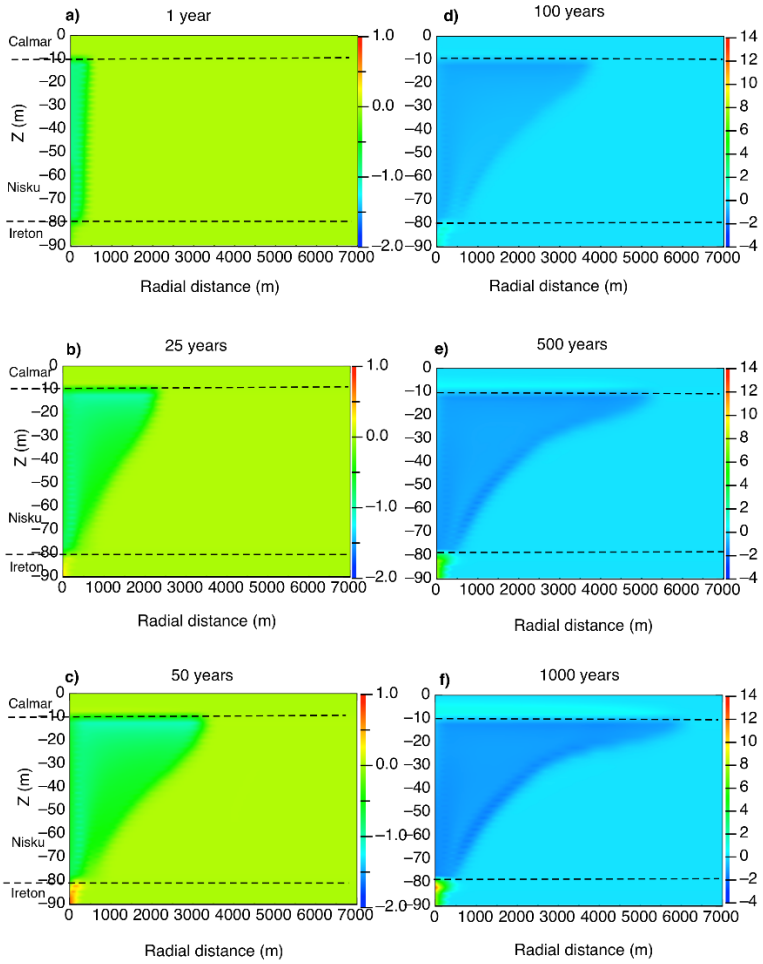

Figure 4: Spatial distribution of CO2 sequestered (kg/m^3 rock) as minerals (SMco2).

Fig. 5 shows the amount of sequestered CO_2 by hydrodynamic and solubility trapping mechanisms in the Nisku Formation over the 1000-year simulation period. The amount of injected CO_2 stored via solubility trapping reached 4.7 Mt after 50 years, and further increased to 11.7 Mt of injected CO_2 after 1000 years. This indicates that 23% of the injected CO_2 was stored via solubility trapping whereas 76% of the injected CO_2 resided still in free supercritical phase in the Nisku aquifer. In the Calmar caprock, the amount of free and dissolved CO_2 was 0.19 and 0.31 Mt, respectively after 1000 years of post-injection (not plotted). The amount of free supercritical and dissolved CO_2 in the Ireton shale was negligible compared to the total injected CO_2 after 1000 years of postinjection (not plotted).

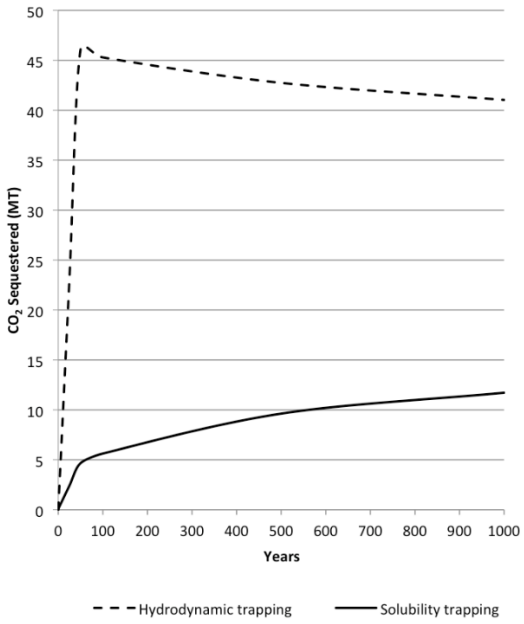

Figure 5: Evolution of CO_2 sequestered in different trapping mechanisms the Nisku aquifer

Prior to CO_2 injection, the porosity and permeability of the Nisku aquifer were 20.9% and 91 mD. Figure 6 displays the changes of porosity and permeability in the Nisku aquifer because of CO_2 injection after 1000 years. The porosity in the Nisku aquifer increased from its initial value of 20.9% up to 21.0% within a radial distance of up to 2.0 km from the injection well. Related permeability in the same radial distance from the injection well increased by 2 mD from its initial value of 91 to 93 mD. These porosity and permeability increases in the Nisku aquifer were associated with the dissolution of dolomite that comprises more than 80% of the Nisku Formation. The overall increase in the porosity and permeability within 2.0 km from the injection well may slightly increase injectivity and the capacity for CO_2 storage. Beyond 2.0 km from the injection well, both porosity and permeability remained unchanged.

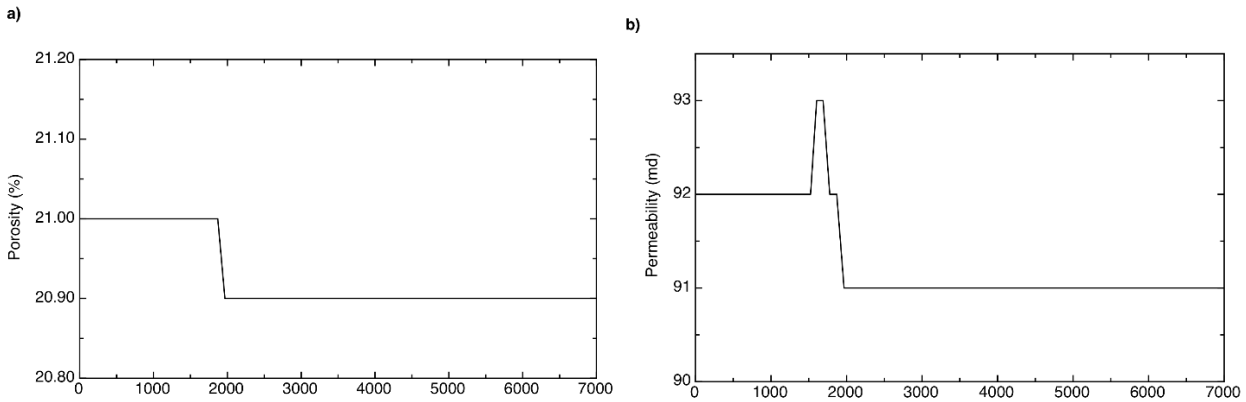

Figure 6: (a) Porosity and (b) Permeability evolution in the Nisku aquifer as a result of mineral reactions after 1000 years of post-injection.

Summary

TOUGHREACT modelling of CO_2 injection into the Devonian Nisku formation has shown that, for an injection rate of 1 Mt/y for 50 y, did not exceed the fracture pressure of both the Nisku and the Calmar caprock. Reactive transport modeling suggests that the overlying Calmar Formation was a good sealing cap rock for the injected CO_2 in the Nisku aquifer.

Approximately 76% of the total injected CO_2 was still present as supercritical CO_2 after 1000 year and hydrodynamically trapped predominantly in the upper 15 m portion of the Nisku Formation. Circa 23% of the injected CO_2 was dissolved in the brine of the Nisku aquifer and retained via solubility trapping after 1000 years. The remaining 1% of the injected CO_2 was sequestered predominantly in the Calmar caprock as free and dissolved CO_2 and to a lesser extent in the underlying Ireton shale partially by mineral trapping due to its high content of weatherable aluminosilicates. Mineral trapping of injected CO_2 in the Nisku aquifer was not observed, because dissolution of dolomite exceeded precipitation of calcite. This resulted in a porosity increase in the Nisku Formation of 0.1% and a permeability increase of 2 mD within a radial distance of ~2.0 km from the injection well. Hence, the risk of decrease or loss of CO_2 injectivity in the Nisku aquifer appears to be minimal during the injection period.

Geochemical modelling using TOUGHREACT allows the evaluation of potential effects injected CO_2 on the reservoir, and caprock. It provides useful information on changes in mineralogy, porosity and permeability of the storage reservoir and caprock. This information along with the other modelling, flow and geomechanical modelling, allows for a determination on the containment potential of the reservoir.

References

Alberta Energy Regulator, 2024, “Directive 65: Resources Applications for Oil and Gas Reservoirs”, https://static.aer.ca/prd/documents/directives/Directive065.pdf

Bachu, S., Gunter, W.D., Perkins, E.H., 1994. Aquifer disposal of CO2: hydrodynamic and mineral trapping. Energy Convers. Manag. 35, 269–279

Bennion, D.B. and Bachu, S. 2007.Permeability and Relative Permeability Measurements at Reservoir Conditions for CO2-Water Systems in Ultra Low Permeability Confining Caprocks. SPE 106995-MS.

Clifford, A.A., 2007. Calculation of Thermodynamic Properties of CO2 using Peng Robinson Equation of State. Critical Processes Ltd.

De Caritat, P., Bloch, J., Hutcheon, I., 1994. LPNORM: a linear programming normative analysis code. Comput. Geosci. 20, 313–347.

Gunter, W.D., Perkins, E.H., McCann, T.J., 1993. Aquifer disposal of CO2-rich gases: reaction design for added capacity. Energy Convers. Manag. 34, 941–948.

Gunter, W.D., Bachu, S., Law, D.H.S., Marwaha, V., Drysdale, D.L., MacDonald, D.E., McCann, T.J., 1996. Technical and economic feasibility of CO2 disposal in aquifers within the Alberta Sedimentary Basin, Canada. Energy Convers. Manag. 37, 1135–1142.

Gunter, W.D., Wiwchar, B., Perkins, E.H., 1997. Aquifer disposal of CO2-rich greenhouse gases: extension of the time scale of experiment for CO2-sequestering reactions by geochemical modeling. Mineral. Petrol. 59, 121–140.

Hitchon, B. (Ed.), 1996. Aquifer Disposal of Carbon Dioxide. Geoscience Publishing, Ltd, Sherwood Park, Alberta, Canada.

Lasaga, A.C., Soler, J.M., Ganor, J., Burch, T.E., Nagy, K.L., 1994. Chemical weathering rate laws and global geochemical cycles. Geochimica et Cosmochimica Acta 58, 2361–2386.

Lavoie, R., Keith, D., 2010. Wabamun Area CO2 Sequestration Project (WASP) – Executive Summary Report, http://www.ucalgary.ca/wasp/Executive%20Summary.pdf

Lindeberg, E. Bergamo, P. 2002. SINTEF Petroleum Research Report. http://www.entek.chalmers.se/~anly/presentations/Long-term%20fate%20of%20CO2.pdf

Narasimhan, T.N., Witherspoon, P.A., 1976. An integrated finite difference method for analyzing fluid flow in porous media. Water Resour. Res. 12, 57–64.
Nightingale, M., Shevalier, M., Mayer, B., 2009. Wabamun Area Sequestration Project: Mineralogy Report. Wabamum Area CO2 Sequestration Project (WASP) Internal Report. University of Calgary.
Palandri, J., Kharaka, Y.K., 2004. A compilation of rate parameters of water–mineral interaction kinetics for application to geochemical modeling. Open File Report 2004-1068, U.S. Geological Survey, Menlo Park, CA, 64.
Pruess, K., 1991. TOUGH2: A General Numerical Simulator for Multiphase Fluid and Heat Flow, Lawrence Berkeley Laboratory Report LBL-29400, Berkeley, California.
Shevalier, M., Mayer, B., 2009. Wabamun Area Sequestration Project: Baseline Geochemistry and Preliminary Geochemical Modelling. Wabamum Area CO2 Sequestration Project (WASP) Internal Report. University of Calgary.
White, C.M., Strazisar, B.R., Granite, E.J., Hoffman, J.S., Pennline, H.W., 2003. J. Air Waste Manage. Assoc. 53, 645–715.
Xu, T., Pruess, K., 1998. Coupled modeling of non-isothermal multiphase flow, solute transport and reactive chemistry in porous and fractured media: 1. Model development and validation. Lawrence Berkeley National Laboratory Report LBNL-42050, Berkeley, California.
Xu, T., Pruess, K., 2001. On fluid flow and mineral alteration in fractured caprock of magmatic hydrothermal systems. J. Geophys. Res. 106, 2121–2138.